Reflection of Nonlinear Waves in Reid's Hysteretic Material: A Numerical Perspective

Pravinkumar R. Ghodake

Dept. of Mechanical Engineering, Indian Institute of Technology Bombay
Mumbai, 400076, Maharashtra, India
mech7pkumar@gmail.com

Abstract. Nonlinear ultrasonics is effective in characterizing early-stage damages in solids. Interaction of a single frequency (*f*) elastic wave with early-stage damages like dislocation substructures, micro-cracks, and micro-voids, etc., generates higher harmonics (*2f, 3f, 4f, 5f,..*). In theoretical and computational studies early-stage damages are modeled as nonlinear material models. Material models such as quadratic, cubic, and hysteretic nonlinearities are commonly implemented in nonlinear wave propagation studies. To understand the interaction of the ultrasonic wave with micro-cracks a pinched hysteretic nonlinearity looks the best fit as it can capture the nonlinear contact mechanisms like opening and closing of micro-cracks which is also known as crack clapping and sliding at the interfaces. One dimensional spatial domain is discretized as a long chain of spring-mass elements. Reid's pinched hysteretic elements are used in a long chain of spring-mass elements for the numerical study of the nonlinear wave propagation through symmetric hysteretic material. Interaction of a single frequency elastic wave with Reid's symmetric hysteretic nonlinearity generates only odd harmonics (*3f, 5f, 7f,…*). Nonlinear reflected waves from both the free and fixed end cases contain only odd harmonics. After reflection, nonlinear wave transfers energy from 5^{th} and 7^{th} harmonics to 3^{rd} harmonics. Pinched hysteretic loops are observed corresponding to both the incident and reflected wave. The pinching at the origin of the hysteretic loops gets opened due to the reflection of nonlinear waves. Evolving pinched hysteretic loops are observed due to Gaussian pulse as an input pulse whereas repetitive pinched hysteretic loops are observed due to sine pulse as an input pulse. In one-way two-wave mixing, both incident and reflected waves from free and fixed ends contain sum and difference frequency harmonics along with the corresponding odd harmonics of input frequencies. Reflected waves transfer energy from the frequency combinations present near 5^{th} harmonics to frequency combinations present near 3^{rd} harmonics. Minor hysteretic loops due to wave mixing are observed within the major pinched hysteresis loops. As this numerical study is simple in understanding, formulation, and implementation, it will help to solve inverse problems in nonlinear waves with less computational resources and within a short time.

Keywords: nonlinear waves, wave-mixing, pinched hysteresis, nonlinear ultrasonics

1 Introduction

In practice, mechanical components and structures are subjected to complex loadings such as fatigue and creep most of the time. Fatigue and creep degrades the material properties continuously. This degradation is known as damage inside solid materials. The damages are mainly considered as early-stage damages at micro-scale and macro-scale damages at later stages of the loading [1]. In structural health monitoring, damage detection is an important step. Linear ultrasonics can be used effectively to detect the damage level and type of damages at a macro-scale, but it is insensitive to micro-scale damages. It has been reported by various studies that the nonlinear ultrasonics technique has the potential to detect microscale damages, which will be helpful to get an early warning of the material damage. Early-stage damages take nearly 80-90% of the total life of the components when the metallic components are under fatigue and creep loading [2]. In metals, the early-stage damage includes an appearance of the dislocations and combining dislocations to generate dislocation substructures like veins and

persistent slip bands, and these substructures get accumulated at the grain boundaries to introduce local plasticity, and then they produce micro-cracks [3]. In nonlinear ultrasonics, interaction of a single frequency (*f*) ultrasonic pulse generates higher harmonics (*2f, 3f, 4f, 5f,..*), also known as a harmonic generation. Theoretical, computational, and experimental studies showed that the amplitudes of the higher harmonics can be directly correlated to the damage level present in the solid [2].

In theoretical and computational studies early-stage damages are modeled as quadratic, cubic, and hysteretic nonlinear material. Perturbation methods are used to get an approximate analytical solution of the incident or forward propagating waves in nonlinear materials. For reflected waves in quadratic nonlinear material theoretical solution is given by Bender et.al [4]. As obtaining an analytical solution for the reflected nonlinear waves in hysteretic nonlinear material is challenging, a numerical study on the reflection of the nonlinear wave in hysteretic material is conducted. Understanding the interaction of ultrasonic waves mainly with micro-cracks by modeling them using numerical methods like finite difference method, finite element method, finite integration method in 2-D domain takes significant computational power and time in comparison with 1-D models and this proposed implementation. The nonlinearity introduced due to micro-cracks is also known as contact acoustic nonlinearity (CAN) because of closing and opening of micro-cracks and full/partial sliding at the contact interface as shown in many simulations [5-9] and experiments [5],[10-11]. To reduce computational efforts and the complexity of the problem formulation and implementation, here in this research study a one-dimensional domain is discretized as the long chain of spring-mass elements along with Reid's hysteretic elements [12] added in parallel to capture the pinched hysteretic behavior due to micro-cracks (Fig. 1). In this article, the reflection of the nonlinear waves in pinched rate-independent Reid's hysteretic material is studied numerically. In section 2 numerical model is presented, in section 3 results are discussed in detail. Conclusions are drawn in section 4.

2 Numerical model

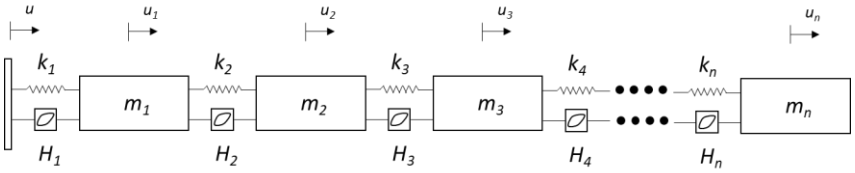

Figure 1. Schematic of long spring-mass chain with hysteretic elements

A one-dimensional domain is assumed as a long chain of spring-mass elements (Fig. 1) with masses $m_1 = m_2 = ... = m$ and stiffness $k_1 = k_2 = ... = k$ to model linear material. Hysteretic nonlinearity is added in parallel to linear springs by adding hysteretic elements $H_1 = H_2 = ... = H$. Reid's hysteretic element [12] is considered in this study, as most of the micro-cracks closing and opening behavior also known as crack clapping phenomenon can be well characterized by the triangular hysteretic curves [13]. The force of Reid's single hysteretic element *H* is given as follows

$$z = k_H[\eta\ sgn(u\dot{u})u] \tag{1}$$

The input displacement *u* is given at the left end of the chain as shown in Fig. 1. In experiments, both the sinusoidal and Gaussian pulses are used as shown in Fig. 2(a) and Fig. 2(c) for single frequency wave input given as

$$\mathrm{u} = \mathrm{A}\sin(2\pi f t) \tag{2}$$

for sine pulse (Fig. 2(a)) and

$$\mathrm{u} = 0.5\ \mathrm{A}\ [1 - \cos(2\pi f t/N)]\sin(2\pi f t) \tag{3}$$

for Gaussian pulse (Fig. 2(c)). To avoid unwanted harmonics generated during nonlinear ultrasonic experiments due to system nonlinearity wave-mixing technique is preferred. A single pulse with two input frequencies (Fig. 2(b) and Fig. 2(d)) is sent from the left end domain. This is also known as one-way two-wave mixing. From now onwards terms wave mixing and one-way two-wave will be used interchangeably. The expression for wave mixing of sinusoidal waves (Fig. 2(b)) is given as

$$\mathrm{u} = A_1\sin(2\pi f_1 t) + A_2\sin(2\pi f_2 t) \tag{4}$$

Similarly, we can write for mixed Gaussian pulse (Fig. 2(d)) as

$$\begin{aligned} u = {} & 0.5\, A_1\, [1 - \cos(2\pi f_1 t/N)] \sin(2\pi f_1 t) \\ & + 0.5\, A_2\, [1 - \cos(2\pi f_2 t/N)] \sin(2\pi f_2 t) \end{aligned} \tag{5}$$

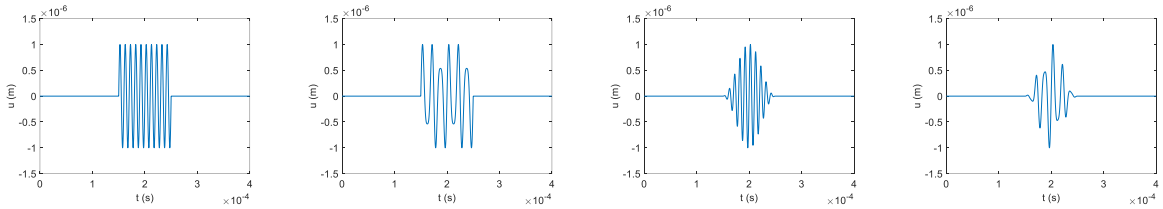

a) Single-frequency sine b) Mixed sine c) Single-freq. Gaussian d) Mixed Gaussian

Figure 2. Input short pulses

A sufficient number of masses (800) are considered to avoid reflections of the waves at the left end of the chain. Two different case studies are carried out: a) free right end and b) fixed right end of the chain. The displacement of the end mass is kept zero in the case of the fixed end study and kept free in the case of the free end study. Stability and convergence of the numerical study are ensured by selecting appropriate time stepping loosely based on the CFL condition. MATLAB inbuilt ode solver is used to solve the system of equations. The material properties used in this study are noted in Tab. 1. The incident and reflected waves are noted independently and then analyzed for frequency response and hysteretic curves at 400th mass. The results are discussed in the next section.

Table 1. Material properties used in the numerical study

m (kg)	k (MN/m)	k_H (KN/m)	η
1.3e-6	38.5	38.5	0.3

3 Results and Discussion

The results for fixed end and free end cases are plotted as frequency responses and hysteretic curves. In all the frequency responses a power spectrum is plotted with dB scale on the y-axis and frequency on the x-axis (e.g. Fig. 3(a)). Normalized input displacement versus normalized hysteretic force is plotted to understand the nature of the hysteretic curves as seen in Fig. 3(b). Frequency responses have significant importance in the acoustics community to understand the early-stage damage level and hysteretic curves have importance mainly in the applied mechanics community to understand the type of hysteresis and local damages like here in this particular study the focus is on hysteresis due to micro-cracks.

3.1 Free end

Frequency response for a single frequency (f = 0.1 MHz) incident sine pulse (Fig. 2(a)) at 400th mass shows the generation of only odd harmonics (*3f, 5f, 7f,…*) as seen from Fig. 3(a). Triangular pinched hysteretic curves are observed (Fig. 3(b)). Similarly, in the case of reflected wave at 400th mass only odd harmonics are present in frequency response (Fig. 3(c)). Interestingly, the opening of the previously pinched hysteretic loop is observed at the center (Fig. 3(d)), but the loops are pinched at other positions resulting in three closed loops and all the loops are symmetric about the diagonal of the graph ($z = u$). When a single frequency Gaussian pulse (Fig. 2(c)) is sent through the hysteretic material, both the incident (Fig. 3(e)) and reflected (Fig. 3(g)) waves contain only odd harmonics. The frequency response of Gaussian pulse input has sufficiently fewer small oscillations than sine pulse input and broader distribution near the peaks of the harmonics as the Gaussian pulse is a broadband pulse. Fig. 3(f) shows evolving triangular pinched hysteretic loops of an incident wave at 400th mass from smaller loop size to larger loop size then again back to the smaller loop size. Similarly, evolving hysteretic loops of reflected waves are observed where the pinching at the center is opened and three closed loops are generated with pinching at the other two locations. Most importantly, comparing amplitudes of higher harmonics of the incident

wave and reflected wave (comparing Fig. 3(a) and Fig. 3(c) or Fig. 3(e) and Fig. 3(e)), the amplitudes of 5^{th} and 7^{th} harmonics of the incident wave decreases when we receive the reflected wave at the same location (400^{th} mass), but the amplitude of 3^{rd} harmonics of the reflected wave increases in comparison with the 3^{rd} harmonics of the incident wave. From this observation, we can conclude that upon reflection the energy from the 5^{th} and 7^{th} harmonics gets transferred to only 3^{rd} harmonics (first odd harmonics).

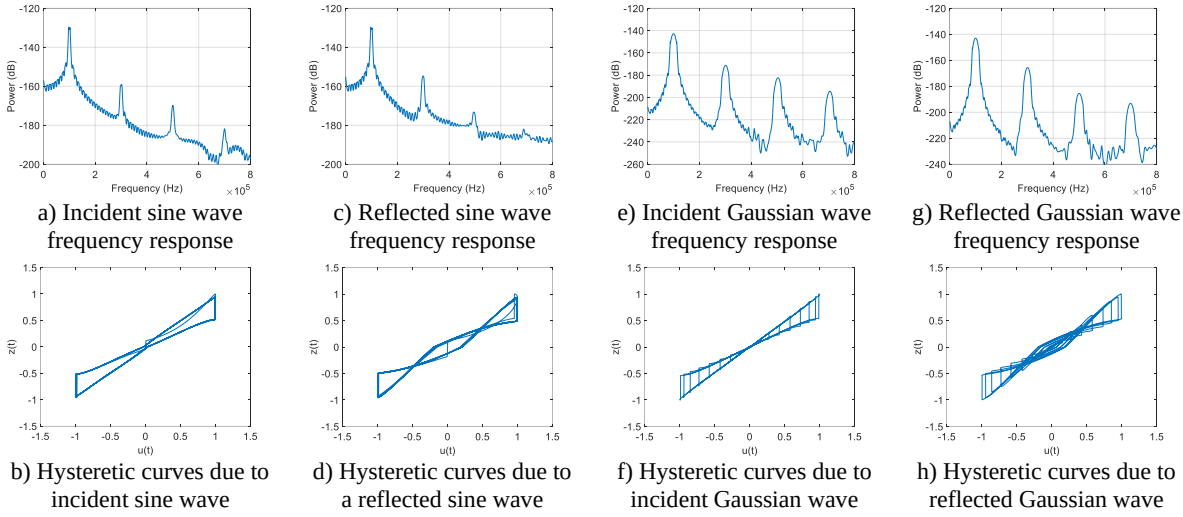

a) Incident sine wave frequency response | c) Reflected sine wave frequency response | e) Incident Gaussian wave frequency response | g) Reflected Gaussian wave frequency response

b) Hysteretic curves due to incident sine wave | d) Hysteretic curves due to a reflected sine wave | f) Hysteretic curves due to incident Gaussian wave | h) Hysteretic curves due to reflected Gaussian wave

Figure 3. Frequency response and hysteretic curves at 400^{th} mass due to single-frequency wave input in 1-D rod with a free end

In one-way two-wave mixing nonlinear ultrasonic testing, a single pulse with two input frequencies is sent from only one side of the spatial domain (left end of the chain). To conduct same one-way two-wave mixing numerical experiment, mixed pulse with two input frequencies ($f_1 = 0.06$ *MHz* and $f_2 = 0.1$ *MHz*) is sent (Fig. 1(b) and Fig. (d)). Here in this particular study the amplitude ratio $A_1/A_2 = 3$ is used in Eq. 5. This can be seen in the frequency response (note that this is power spectrum) plot shown in Fig. 4(a), where amplitude at 0.06 MHz frequency is higher than the amplitude at 0.1 MHz frequency.

Table 2. Frequency combinations (10^5 Hz) due to one-way two-wave mixing ($f_1 = 0.06$ *MHz* and $f_2 = 0.1$ *MHz*)

$2f_1 - f_2$ = **0.2**	$2f_1 + f_2$ = **2.2**	$6f_1 - f_2$ = **4.6**	$6f_1 + f_2$ = **2.6**	$3f_1$ = **1.8**	$11f_1$ = **6.6**	$3f_2$ = **3.0**
$f_1 - 2f_2$ = **1.4**	$f_1 + 2f_2$ = **2.6**	$f_1 - 6f_2$ = **6.6**	$f_1 + 6f_2$ = **5.4**	$5f_1$ = **3.0**	$13f_1$ = 7.8	$5f_2$ = **5.0**
$4f_1 - f_2$ = **1.4**	$4f_1 + f_2$ = **3.4**	$8f_1 - f_2$ = **3.8**	$8f_1 + f_2$ = **5.8**	$7f_1$ = **4.2**		$7f_2$ = **7.0**
$f_1 - 4f_2$ = **3.4**	$f_1 + 4f_2$ = **4.6**	$f_1 - 8f_2$ = **7.4**	$f_1 + 8f_2$ = 8.6	$9f_1$ = **5.4**		$9f_2$ = 9.0

In general, due to one-way two-wave mixing sum ($f_1 + f_2$, $2f_1 + f_2$, $f_1 + 2f_2$, $3f_1 + f_2$, $f_1 + 3f_2$, ...) and difference ($f_1 - f_2$, $2f_1 - f_2$, $f_1 - 2f_2$, $3f_1 - f_2$, $f_1 - 3f_2$, ...) frequencies are observed along with the corresponding higher harmonics of the input frequencies ($2f_1$, $2f_2$, $3f_1$, $3f_2$, $4f_1$, $4f_2$, $5f_1$, $5f_2$, $6f_1$, $6f_2$, ...). One-way two-wave mixing in Reid's pinched hysteretic nonlinear material gives only those sum and difference frequency combinations whose net difference is an odd multiplier e.g., $2f_1 - f_2$ but not $3f_1 - f_2$. All the observed possible sum and difference frequencies along with the only odd higher harmonics corresponding to both the input frequencies are noted in Tab. 2 and can be verified from the frequency responses shown in Fig. 4(a), Fig. 4(c), Fig. 4(e), and Fig. 4(g) for both incident and reflected waves. Triangular hysteretic pinched loops due to incident waves are observed as seen from Fig. 4(b). Comparing hysteretic loops due to single-frequency incident wave (Fig. 3(b)) with hysteretic loops due to mixed incident wave (Fig. 4(b) and Fig. 4(f)) shows that, additional small loops [14] are introduced due to mixing. Hysteretic loops due to reflected wave show opening of the pinching at the center and introducing two more pinching points (Fig. 4(d) and Fig. 4(h)).

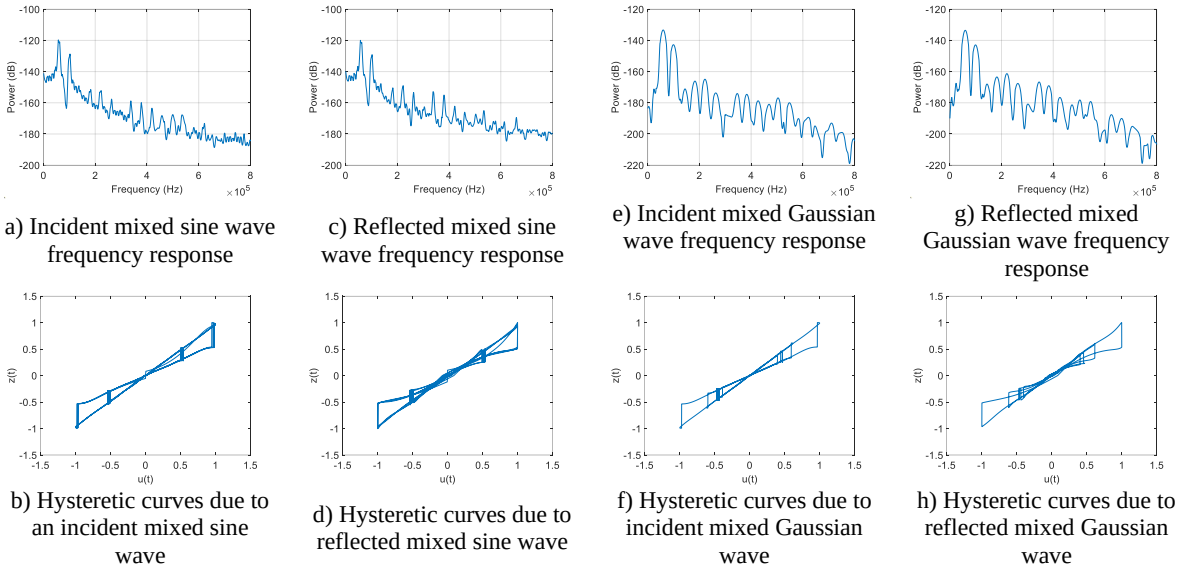

a) Incident mixed sine wave frequency response

c) Reflected mixed sine wave frequency response

e) Incident mixed Gaussian wave frequency response

g) Reflected mixed Gaussian wave frequency response

b) Hysteretic curves due to an incident mixed sine wave

d) Hysteretic curves due to reflected mixed sine wave

f) Hysteretic curves due to incident mixed Gaussian wave

h) Hysteretic curves due to reflected mixed Gaussian wave

Figure 4. Frequency response and hysteretic curves at 400th mass due to one-way two-wave mixing in 1-D rod with a free end

3.2 Fixed end

Similar to the free end case, the frequency responses of both single frequency incident and reflected waves contain only odd harmonics. After reflection, a decrease in amplitudes of the 5th and 7th harmonics shows energy transfer from 5th and 7th harmonics to only 3rd harmonics (Fig. 5(a), Fig. 5(c), Fig. 5(e), and Fig. (g)). As the other end is fixed, the wave will reflect with 180^0 phase difference. Due to phase change, the hysteretic loops of the reflected wave are rotated by 90^0 in hysteretic curves space (Fig. 5(d) and Fig. 5(h)). Similar to the free end case in one-way two-wave wave mixing, sum, and difference frequency combinations are noted along with the corresponding odd harmonics as mentioned in Tab. 2 and as seen from Fig. 6(a), Fig. 6(c), Fig. 5(e), and Fig. 5(g). Due to 180^0 phase change, the hysteretic loops of reflected waves are rotated by 90^0 in a hysteretic curves space.

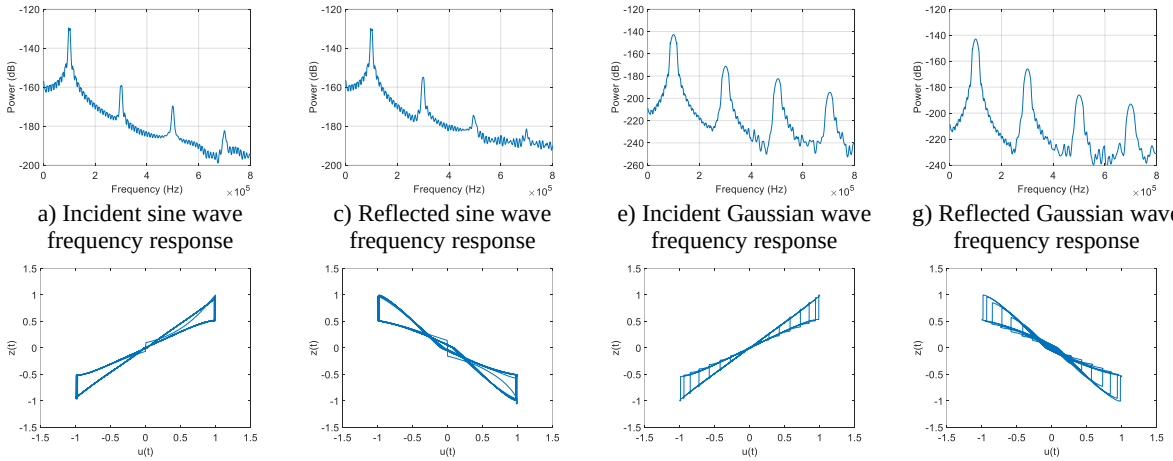

a) Incident sine wave frequency response

c) Reflected sine wave frequency response

e) Incident Gaussian wave frequency response

g) Reflected Gaussian wave frequency response

b) Hysteretic curves due to incident sine wave

d) Hysteretic curves due to a reflected sine wave

f) Hysteretic curves due to incident Gaussian wave

h) Hysteretic curves due to reflected Gaussian wave

Figure 5. Frequency response and hysteretic curves at 400th mass due to single-frequency wave input in 1-D rod with a fixed end

To get quantitative insight into frequency responses, magnitudes of the higher harmonics amplitudes are converted from dB to power units, and the ratios of the harmonic amplitudes of the reflected and incident waves are defined as R/I as seen from legends of Fig. 7 and Fig. 8. The fundamental amplitude ratio in free and fixed end

cases is nearly the same for both the sine and Gaussian input pulses. The amplitude ratio (R/I) at the 3rd harmonics (first odd harmonics) is nearly 3.5 times higher than the fundamental amplitude ratio. The amplitude ratio of the 7th harmonics is nearly 1.5 times higher than the fundamental amplitude ratio. Interestingly, the amplitude ratio of the 5th harmonics (second odd harmonics) is less than (nearly 0.5 times) the fundamental amplitude ratio. The amplitude ratios for the fixed end case at 3rd, 5th, and 7th harmonics are slightly lesser than the amplitude ratio of the free end case. Amplitude ratios at 3rd harmonics due to sine pulse input are lesser than the Gaussian pulse input but it's the other way round at 5th and 7th harmonics.

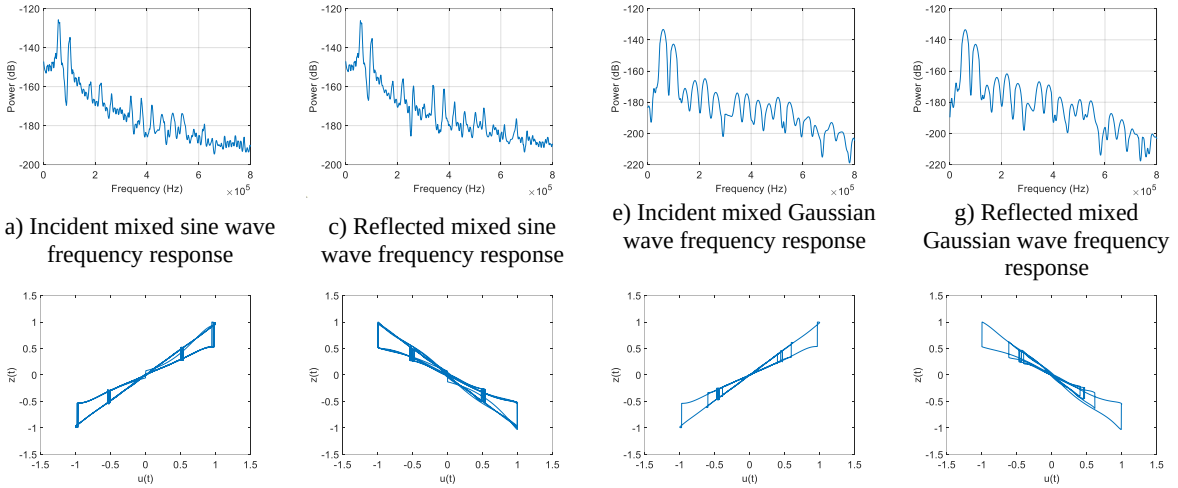

a) Incident mixed sine wave frequency response

c) Reflected mixed sine wave frequency response

e) Incident mixed Gaussian wave frequency response

g) Reflected mixed Gaussian wave frequency response

b) Hysteretic curves due to an incident mixed sine wave

d) Hysteretic curves due to reflected mixed sine wave

f) Hysteretic curves due to incident mixed Gaussian wave

h) Hysteretic curves due to reflected mixed Gaussian wave

Figure 6. Frequency response and hysteretic curves at 400th mass due to one-way two-wave mixing in 1-D rod with a fixed end

In one-way two-wave mixing, a wide range of amplitude ratios (R/I) are obtained for sum, difference, and corresponding odd harmonics as shown in Fig. 8. The amplitude ratios at fundamental input frequencies (0.06 and 0.1 MHz) are of the same value in fixed and free end cases for both sine and Gaussian pulse inputs. Amplitude ratios up to 5th harmonics due to sine pulse are slightly less in magnitude than the amplitude ratios due to Gaussian input pulse. Two maximum value peaks are observed at 0.34 and 0.66 MHz frequencies in Gaussian input pulse. Interestingly, the amplitude ratio at 0.02 MHz (subharmonics) due to Gaussian pulse is nearly 2 times higher than the amplitude ratio due to sine input pulse. Comparing Fig. 7 and Fig. 8 we can broadly conclude that both in a single wave and wave-mixing cases the energy from the 5th harmonics and its neighborhood harmonics gets transferred to 3rd harmonics and the neighborhood harmonics due to reflected waves. Understanding such energy transfer is very important and helpful for the selection of input frequencies and targeting dominant frequency combinations due to one-way two-wave mixing.

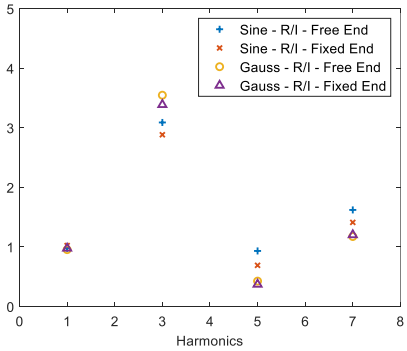

Figure 7. Reflected to incident (R/I) wave amplitude ratios corresponding to observed harmonics at 400th mass due to single-frequency wave input

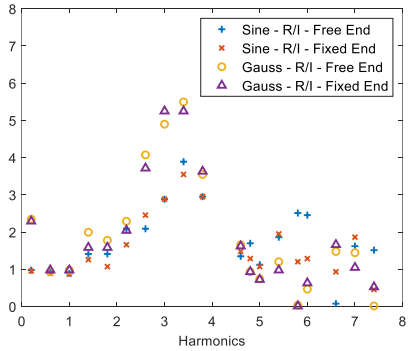

Figure 8. Reflected to incident (R/I) wave amplitude ratios corresponding to observed harmonics at 400th mass due to one-way two-wave mixing

4 Conclusions

Interaction of a single frequency wave with Reid's hysteretic material generates only odd harmonics both in the case of an incident and a reflected wave from a free and fixed end. The hysteretic curves obtained are pinched at the center for an incident wave but in the case of the reflected wave, the pinching is opened at the center resulting in adding two pinching points at positions other than the center. The orientation of hysteretic loops of reflected waves at the fixed end gets rotated by 90^0 in comparison with the hysteretic loops due to incident waves. Sum and difference frequencies along with the corresponding odd harmonics are observed due to one-way two-wave mixing in pinched hysteretic material. The amplitude ratio gives more insight into the redistribution of the harmonic energy within the incident and reflected pulses. In a single frequency input pulse, energy from the 5^{th} and 7^{th} harmonics is transferred to the 3^{rd} harmonics as the wave gets reflected. The amount of energy transferred from only the 5^{th} harmonics (second odd harmonics) to the 3^{rd} harmonics (first odd harmonics) is significant. Similarly, in wave mixing the energy from the frequency combinations present near 5^{th} harmonics is transferred to frequency combinations present near 3^{rd} harmonics when a wave gets reflected in a nonlinear pinched hysteretic material.

Simple formulation, fewer computational resources required and short computational time makes this study useful in solving nonlinear inverse problems in nonlinear ultrasonics for in-situ and ex-situ structural health monitoring applications. Initial quick computational studies will help in the selection of input pulse amplitude and frequency combinations and target the possible frequency combinations for nonlinear pulse-echo experiments in pinched hysteretic materials.

Acknowledgements. I would like to thank the Acoustical Society of America (ASA) for supporting me through the CIRE student grant. I thank Saurabh Biswas for the discussions.

Authorship statement. The author hereby confirm that he is the sole liable person responsible for the authorship of this work, and that all material that has been herein included as part of the present paper is either the property (and authorship) of the author, or has the permission of the owner to be included here.

References

[1] V. Aleshin, S. Delrue, A. Trifonov, O. Bou, and K. Van Den Abeele, "Two dimensional modeling of elastic wave propagation in solids containing cracks with rough surfaces and friction – Part I : Theoretical background," Ultrasonics, vol. 82, pp. 11–18, 2018.
[2] P. B. Nagy, "Fatigue damage assessment by nonlinear materials characterization," Ultrasonics, vol. 36, pp. 375–381, 1998.
[3] J. H. Cantrell, "Substructural organization, dislocation plasticity and harmonic generation in cyclically stressed wavy slip metals," Proc. R. Soc. A Math. Phys. Eng. Sci., vol. 460, no. 2043, pp. 757–780, 2004.
[4] F. A. Bender, J. Y. Kim, L. J. Jacobs, and J. Qu, "The generation of second harmonic waves in an isotropic solid with quadratic nonlinearity under the presence of a stress-free boundary," Wave Motion, vol. 50, no. 2, pp. 146–161, 2013.
[5] M. Hong, Z. Su, Q. Wang, L. Cheng, and X. Qing, "Modeling nonlinearities of ultrasonic waves for fatigue damage characterization: Theory, simulation, and experimental validation," Ultrasonics, vol. 54, no. 3, pp. 770–778, 2014.
[6] G. P. M. Fierro, F. Ciampa, D. Ginzburg, E. Onder, and M. Meo, "Nonlinear ultrasound modelling and validation of fatigue damage," J. Sound Vib., vol. 343, pp. 121–130, 2015.
[7] X. Ding et al., "Generation mechanism of nonlinear Rayleigh surface waves for randomly distributed surface micro-cracks," Materials (Basel)., vol. 11, no. 4, 2018.
[8] X. Wan, Q. Zhang, G. Xu, and P. W. Tse, "Numerical Simulation of Nonlinear Lamb Waves Used in a Thin Plate for Detecting Buried Micro-Cracks," Sensors, vol. 14, pp. 8528–8546, 2014.
[9] J. Melchor, W. J. Parnell, N. Bochud, L. Peralta, and G. Rus, "Damage prediction via nonlinear ultrasound: a micro-mechanical approach," Ultrasonics, no. October, 2018.
[10] J. H. Cantrell and W. Yost, "Nonlinear ultrasonic characterization of fatigue microstructures," Int. J. Fatigue, vol. 23, pp. 487–490, 2001.
[11] J. Jiao, H. Lv, C. He, and B. Wu, "Fatigue crack evaluation using the non-collinear wave mixing technique," Smart Mater. Struct., vol. 26, no. 6, 2017.
[12] T. J. Reid, "Free Vibration and Hysteretic Damping," J. R. Aeronaut. Soc., vol. 60, no. 544, pp. 283–283, Apr. 1956.
[13] S. Biswas, P. Jana, and A. Chatterjee, "Hysteretic damping in an elastic body with frictional microcracks," Int. J. Mech. Sci., vol. 108–109, pp. 61–71, 2016.
[14] P. R. Ghodake and S. Biswas, "Wave propagation in a one-dimensional bar with rate-independent hysteresis," J. Acoust. Soc. Am., vol. 148, no. 4, 2020.